



**HAL**  
open science

# Querying RDF Data Using A Multigraph-based Approach

Vijay Ingalalli, Dino Ienco, Pascal Poncelet, Serena Villata

► **To cite this version:**

Vijay Ingalalli, Dino Ienco, Pascal Poncelet, Serena Villata. Querying RDF Data Using A Multigraph-based Approach. EDBT 2016 - 19th International Conference on Extending Database Technology, Mar 2016, Bordeaux, France. pp.245-256, 10.5441/002/edbt.2016.24 . lirmm-01245146

**HAL Id: lirmm-01245146**

**<https://hal-lirmm.ccsd.cnrs.fr/lirmm-01245146v1>**

Submitted on 16 Dec 2015

**HAL** is a multi-disciplinary open access archive for the deposit and dissemination of scientific research documents, whether they are published or not. The documents may come from teaching and research institutions in France or abroad, or from public or private research centers.

L'archive ouverte pluridisciplinaire **HAL**, est destinée au dépôt et à la diffusion de documents scientifiques de niveau recherche, publiés ou non, émanant des établissements d'enseignement et de recherche français ou étrangers, des laboratoires publics ou privés.



Distributed under a Creative Commons Attribution - NonCommercial - NoDerivatives 4.0 International License

# Querying RDF Data Using A Multigraph-based Approach

Vijay Ingalalli  
LIRMM, IRSTEA  
Montpellier, France  
vijay@lirmm.fr

Dino Ienco  
IRSTEA  
Montpellier, France  
dino.ienco@irstea.fr

Pascal Poncelet  
LIRMM  
Montpellier, France  
pascal.poncelet@lirmm.fr

Serena Villata  
INRIA  
Sophia Antipolis, France  
serena.villata@inria.fr

## ABSTRACT

RDF is a standard for the conceptual description of knowledge, and SPARQL is the query language conceived to query RDF data. The RDF data is cherished and exploited by various domains such as life sciences, Semantic Web, social network, etc. Further, its integration at Web-scale compels RDF management engines to deal with complex queries in terms of both size and structure. In this paper, we propose AMBER (Attributed Multigraph Based Engine for RDF querying), a novel RDF query engine specifically designed to optimize the computation of complex queries. AMBER leverages subgraph matching techniques and extends them to tackle the SPARQL query problem. First of all RDF data is represented as a multigraph, and then novel indexing structures are established to efficiently access the information from the multigraph. Finally a SPARQL query is represented as a multigraph, and the SPARQL querying problem is reduced to the subgraph homomorphism problem. AMBER exploits structural properties of the query multigraph as well as the proposed indexes, in order to tackle the problem of subgraph homomorphism. The performance of AMBER, in comparison with state-of-the-art systems, has been extensively evaluated over several RDF benchmarks. The advantages of employing AMBER for complex SPARQL queries have been experimentally validated.

## 1. INTRODUCTION

In the recent years, structured knowledge represented in the form of RDF data has been increasingly adopted to improve the robustness and the performances of a wide range of applications with various purposes. Popular examples are provided by Google, that exploits the so called *knowledge graph* to enhance its search results with semantic information gathered from a wide variety of sources or by Facebook, that implements the so called *entity graph* to empower its search engine and provide further information extracted for instance by Wikipedia. Another example is supplied by re-

cent question-answering systems [4, 14] that automatically translate natural language questions in SPARQL queries and successively retrieve answers considering the available information in the different Linked Open Data sources. In all these examples, complex queries (in terms of size and structure) are generated to ensure the retrieval of all the required information. Thus, as the use of large knowledge bases, that are commonly stored as RDF triplets, is becoming a common way to ameliorate a wide range of applications, efficient querying of RDF data sources using SPARQL is becoming crucial for modern information retrieval systems.

All these different scenarios pose new challenges to the RDF query engines for two vital reasons: firstly, the automatically generated queries cannot be bounded in their structural complexity and size (e.g., the DBPEDIA SPARQL Benchmark [11] contains some queries having more than 50 triplets [2]); secondly, the queries generated by retrieval systems (or by any other applications) need to be efficiently answered in a reasonable amount of time. Modern RDF data management, such as *x-RDF-3X* [12] and *Virtuoso* [6], are designed to address the scalability of SPARQL queries but they still have problems to answer big and structurally complex SPARQL queries [1]. Our experiments with state-of-the-art systems demonstrate that they fail to efficiently manage such kind of queries (Table 1).

Systems	AMBER	<i>gStore</i>	<i>Virtuoso</i>	<i>x-RDF-3X</i>
Time (sec)	1.56	11.96	20.45	>60

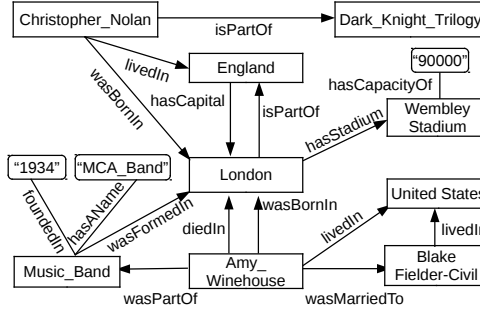
Table 1: Average Time (seconds) for a sample of 200 complex queries on *DBPEDIA*. Each query has 50 triplets.

In order to tackle these issues, in this paper, we introduce AMBER (Attributed Multigraph Based Engine for RDF querying), which is a graph-based RDF engine that involves two steps: an offline stage where RDF data is transformed into multigraph and indexed, and an online step where an efficient approach to answer SPARQL query is proposed. First of all RDF data is represented as a multigraph where subjects/objects constitute vertices and multiple edges (predicates) can appear between the same pair of vertices. Then, new indexing structures are conceived to efficiently access RDF multigraph information. Finally, by representing SPARQL queries also as multigraphs, the query answering task can be reduced to the problem of subgraph homomorphism. To

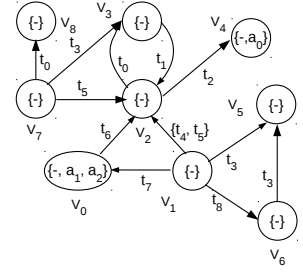
Prefixes: x=<http://dbpedia.org/resource/>; y=<http://dbpedia.org/ontology/>

Subject	Predicate	Object
x:London	y:isPartOf	x:England
x:England	y:hasCapital	x:London
x:Christopher_Nolan	y:wasBornIn	x:London
x:Christopher_Nolan	y:LivedIn	x:England
x:Christopher_Nolan	y:isPartOf	x:Dark_Knight_Triology
x:London	y:hasStadium	x:WembleyStadium
x:WembleyStadium	y:hasCapacityOf	"90000"
x:Amy_Winehouse	y:wasBornIn	x:London
x:Amy_Winehouse	y:diedIn	x:London
x:Amy_Winehouse	y:wasPartOf	x:Music_Band
x:Music_Band	y:hasName	"MCA_Band"
x:Music_Band	y:FoundedIn	"1994"
x:Music_Band	y:wasFormedIn	X:London
x:Amy_Winehouse	y:livedIn	x:United States
x:Amy_Winehouse	y:wasMarriedTo	x:Blake Fielder-Civil
x:Blake Fielder-Civil	y:livedIn	x:United States

(a) RDF triples set



(b) Graph representation of RDF data



(c) Equivalent multigraph  $G$

Figure 1: (a) RDF data in n-triple format; (b) graph representation (c) attributed multigraph  $G$

deal with this problem, AMBER employs an efficient approach that exploits structural properties of the multigraph query as well as the indices previously built on the multigraph structure. Experimental evaluation over popular RDF benchmarks show the quality in terms of time performances and robustness of our proposal.

In this paper, we focus only on the `SELECT/WHERE` clause of the SPARQL language<sup>1</sup>, that constitutes the most important operation of any RDF query engines. It is out of the scope of this work to consider operators like `FILTER`, `UNION` and `GROUP BY` or manage RDF update. Such operations can be addressed in future as extensions of the current work.

The paper is organized as follows. Section 2 introduces the basic notions about RDF and SPARQL language. In Section 3 AMBER is presented. Section 4 describes the indexing strategy while Section 5 presents the query processing. Related works are discussed in Section 6. Section 7 provides the experimental evaluation. Section 8 concludes.

## 2. BACKGROUND AND PRELIMINARIES

In this section we provide basic definitions on the interplay between RDF and its multigraph representation. Later, we explain how the task of answering SPARQL queries can be reduced to multigraph homomorphism problem.

### 2.1 RDF Data

As per the W3C standards<sup>2</sup>, RDF data is represented as a set of triples  $\langle S, P, O \rangle$ , as shown in Figure 1a, where each triple  $\langle s, p, o \rangle$  consists of three components: a *subject*, a *predicate* and an *object*. Further, each component of the RDF triple can be of any two forms; an *IRI* (Internationalized Resource Identifier) or a literal. For brevity, an *IRI* is usually written along with a prefix (e.g., `<http://dbpedia.`

`org/resource/isPartOf>` is written as `'x:isPartOf'`), whereas a literal is always written with inverted commas (e.g., `"90000"`). While a subject  $s$  and a predicate  $p$  are always an *IRI*, an object  $o$  is either an *IRI* or a literal.

RDF data can also be represented as a directed graph where, given a triple  $\langle s, p, o \rangle$ , the subject  $s$  and the object  $o$  can be treated as vertices and the predicate  $p$  forms a directed edge from  $s$  to  $o$ , as depicted in Figure 1b. Further, to underline the difference between an *IRI* and a literal, we use standard rectangles and arc for the former while we use beveled corner and edge (no arrows) for the latter.

#### 2.1.1 Data Multigraph Representation

Motivated by the graph representation of RDF data (Figure 1b), we take a step further by transforming it to a data multigraph  $G$ , as shown in Figure 1c.

Let us consider an RDF triple  $\langle s, p, o \rangle$  from the RDF triples set  $\langle S, P, O \rangle$ . Now to transform the RDF triples set into data multigraph  $G$ , we set four protocols: we always treat the subject  $s$  as a vertex; a predicate  $p$  is always treated as an edge; we treat the object  $o$  as a vertex only if it is an *IRI* (e.g., vertex  $v_2$  corresponds to object `'x:London'`); when the object is a literal, we combine the object  $o$  and the corresponding predicate  $p$  to form a tuple  $\langle p, o \rangle$  and assign it as an attribute to the subject  $s$  (e.g., `<'y:hasCapacityOf', '90000'>` is assigned to vertex  $v_4$ ). Every vertex is assigned a null value `{-}` in the attribute set. However, to realize this in the realms of graph management techniques, we maintain three different dictionaries, whose elements are a pair of 'key' and 'value', and a mapping function that links them. The three dictionaries depicted in Table 2 are: a vertex dictionary (Table 2a), an edge-type dictionary (Table 2b) and an attribute dictionary (Table 2c). In all the three dictionaries, an RDF entity represented by a 'key' is mapped to a corresponding 'value', which can be a vertex/edge/attribute identifier. Thus by using the mapping functions -  $\mathcal{M}_v$ ,  $\mathcal{M}_e$ , and  $\mathcal{M}_a$  for vertex, edge-type and attribute mapping respec-

<sup>1</sup><http://www.w3.org/TR/sparql11-overview/>

<sup>2</sup><http://www.w3.org/TR/2014/REC-rdf11-concepts-20140225/>

tively, we obtain a directed, vertex attributed data multigraph  $G$  (Figure 1c), which is formally defined as follows.

**DEFINITION 1.** Directed, Vertex Attributed Multigraph. *A directed, vertex attributed multigraph  $G$  is defined as a 4-tuple  $(V, E, L_V, L_E)$  where  $V$  is a set of vertices,  $E \subseteq V \times V$  is a set of directed edges with  $(v, v') \neq (v', v)$ ,  $L_V$  is a labelling function that assigns a subset of vertex attributes  $A$  to the set of vertices  $V$ , and  $L_E$  is a labelling function that assigns a subset of edge-types  $T$  to the edge set  $E$ .*

To summarise, an RDF tripleset is transformed into a data multigraph  $G$ , whose elements are obtained by using the mapping functions as already discussed. Thus, the set of vertices  $V = \{v_0, \dots, v_m\}$  is the set of mapped subject/object *IRI*, and the labelling function  $L_V$  assigns a set of vertex attributes  $A = \{-, a_0, \dots, a_n\}$  (mapped tuple of predicate and object-literal) to the vertex set  $V$ . The set of directed edges  $E$  is a set of pair of vertices  $(v, v')$  that are linked by a predicate, and the labelling function  $L_E$  assigns the set of edge types  $T = \{t_0, \dots, t_p\}$  (mapped predicates) to these set of edges. The edge set  $E$  maintains the topological structure of the RDF data. Further, mapping of object-literals and the corresponding predicates as a set of vertex attributes, results in a compact representation of the multigraph. For example (in Fig. 1c), all the object-literals and the corresponding predicates are reduced to a set of vertex attributes.

## 2.2 SPARQL Query

A SPARQL query usually contains a set of triple patterns, much like RDF triples, except that any of the subject, predicate and object may be a variable, whose bindings are to be found in the RDF data<sup>3</sup>. In the current work, we address the SPARQL queries with ‘SELECT/WHERE’ option, where the predicate is always instantiated as an *IRI* (Figure 2a). The **SELECT** clause identifies the variables to appear in the query results while the **WHERE** clause provides triple patterns to match against the RDF data.

### 2.2.1 Query Multigraph Representation

In any valid SPARQL query (as in Figure 2a), every triplet has at least one unknown variable  $?X$ , whose bindings are to be found in the RDF data. It should now be easy to observe that a SPARQL query can be represented in the form of a graph as in Figure 2b, which in turn is transformed into query multigraph  $Q$  (as in Figure 2c).

In the query multigraph representation, each unknown variable  $?X_i$  is mapped to a vertex  $u_i$  that forms the vertex set  $U$  component of the query multigraph  $Q$  (e.g.,  $?X_6$  is mapped to  $u_6$ ). Since a predicate is always instantiated as an *IRI*, we use the edge-type dictionary in Table 2b, to map the predicate to an edge-type identifier  $t_i \in T$  (e.g., ‘isMarriedTo’ is mapped as  $t_8$ ). When an object  $o_i$  is a literal, we use the attribute dictionary (Table 2c), to find the attribute identifier  $a_i$  for the predicate-object tuple  $\langle p_i, o_i \rangle$  (e.g.,  $\{a_0\}$  forms the attribute for vertex  $u_4$ ). Further, when a subject or an object is an *IRI*, which is a not a variable, we

<sup>3</sup><http://www.w3.org/TR/2008/REC-rdf-sparql-query-20080115/>

$s/o$	$\mathcal{M}_v(s/o)$	$p$	$\mathcal{M}_e(p)$
x:Music_Band	$v_0$	y:isPartOf	$t_0$
x:Amy_Winehouse	$v_1$	y:hasCapital	$t_1$
x:London	$v_2$	y:hasStadium	$t_2$
x:England	$v_3$	y:livedIn	$t_3$
x:WembleyStadium	$v_4$	y:diedIn	$t_4$
x:United States	$v_5$	y:wasBornIn	$t_5$
x:Blake Fielder-Civil	$v_6$	y:wasFormedIn	$t_6$
x:Christopher_Nolan	$v_7$	y:wasPartOf	$t_7$
x:Dark_Knight_Triology	$v_8$	y:wasMarriedTo	$t_8$

(a) Vertex Dictionary	(b) Edge-type Dictionary
$\langle p, o \rangle$	$\mathcal{M}_a(\langle p, o \rangle)$
$\langle y:\text{hasCapacityOf}, \text{“90000”} \rangle$	$a_0$
$\langle y:\text{wasFoundedIn}, \text{“1994”} \rangle$	$a_1$
$\langle y:\text{hasName}, \text{“MCA_Band”} \rangle$	$a_2$

(c) Attribute Dictionary

Table 2: Dictionary look-up tables for vertices, edge-types and vertex attributes

use the vertex dictionary (2a), to map it to an *IRI*-vertex  $u_i^{iri}$  (e.g., ‘x:United\_States’ is mapped to  $u_0^{iri}$ ) and maintain a set of *IRI* vertices  $R$ . Since this vertex is not a variable and a real vertex of the query, we portray it differently by a shaded square shaped vertex. When a query vertex  $u_i$  does not have any vertex attributes associated with it (e.g.,  $u_0, u_1, u_2, u_3, u_6$ ), a null attribute  $\{-\}$  is assigned to it. On the other hand, an *IRI*-vertex  $u_i^{iri} \in R$  does not have any attributes. Thus, a SPARQL query is transformed into a query multigraph  $Q$ .

In this work, we always use the notation  $V$  for the set of vertices of  $G$ , and  $U$  for the set of vertices of  $Q$ . Consequently, a data vertex  $v \in V$ , and a query vertex  $u \in U$ . Also, an incoming edge to a vertex is positive (default), and an outgoing edge from a vertex is labelled negative (‘-’).

## 2.3 SPARQL Querying by Adopting Multigraph Homomorphism

As we recall, the problem of SPARQL querying is addressed by finding the solutions to the unknown variables  $?X$ , that can be bound with the RDF data entities, so that the relations (predicates) provided in the SPARQL query are respected. In this work, to harness the transformed data multigraph  $G$  and the query multigraph  $Q$ , we reduce the problem of SPARQL querying to a sub-multigraph homomorphism problem. The RDF data is transformed into data multigraph  $G$  and the SPARQL query is transformed into query multigraph  $Q$ . Let us now recall that finding SPARQL answers in the RDF data is equivalent to finding all the sub-multigraphs of  $Q$  in  $G$  that are homomorphic. Thus, let us now formally introduce homomorphism for a vertex attributed, directed multigraph.

**DEFINITION 2.** Sub-multigraph Homomorphism. *Given a query multigraph  $Q = (U, E^Q, L_U, L_E^Q)$  and a data multigraph  $G = (V, E, L_V, L_E)$ , the sub-multigraph homomorphism from  $Q$  to  $G$  is a surjective function  $\psi : U \rightarrow V$  such that:*

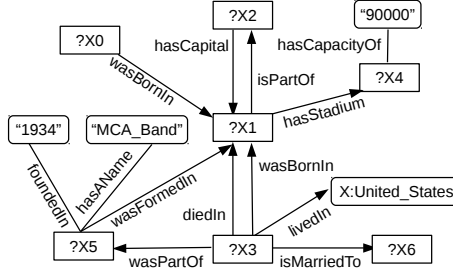
1.  $\forall u \in U, L_U(u) \subseteq L_V(\psi(u))$
2.  $\forall (u_m, u_n) \in E^Q, \exists (\psi(u_m), \psi(u_n)) \in E$ , where  $(u_m, u_n)$  is a directed edge, and  $L_E^Q(u_m, u_n) \subseteq L_E(\psi(u_m), \psi(u_n))$ .

```

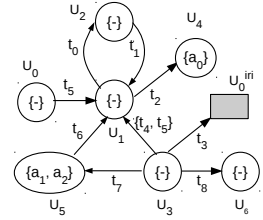
SELECT ?X0 ?X1 ?X2 ?X3 ?X4 ?X5 ?X6 WHERE
?X0 y:livedIn ?X1 .
?X1 y:isPartOf ?X2 .
?X2 y:hasCapital ?X1 .
?X1 y:hasStadium ?X4 .
?X3 y:wasBornIn ?X1 .
?X3 y:diedIn ?X1 .
?X3 y:isMarriedTo ?X6 .
?X3 y:wasPartOf ?X5 .
?X5 y:wasFormedIn ?X1 .
?X4 y:hasCapacity "90000" .
?X5 y:hasName "MCA_Band" .
?X5 y:foundedIn "1934" .
?X3 y:livedIn x:United States .

```

(a) SPARQL Query



(b) Graph representation of SPARQL

(c) Equivalent Multigraph  $Q$ Figure 2: (a) SPARQL query representation; (b) graph representation (c) attributed multigraph  $Q$ 

Thus, by finding all the sub-multigraphs in  $G$  that are homomorphic to  $Q$ , we enumerate all possible homomorphic embeddings of  $Q$  in  $G$ . These embeddings contain the solution for each of the query vertex that is an unknown variable. Thus, by using the inverse mapping function  $\mathcal{M}_v^{-1}(v_i)$  (introduced already), we find the bindings for the SPARQL query. The decision problem of subgraph homomorphism is NP-complete. This standard subgraph homomorphism problem can be seen as a particular case of sub-multigraph homomorphism, where both the labelling functions  $L_E$  and  $L_V^Q$  always return the same subset of edge-types for all the edges in both  $Q$  and  $G$ . Thus the problem of sub-multigraph homomorphism is at least as hard as subgraph homomorphism. Further, the subgraph homomorphism problem is a generic scenario of subgraph isomorphism problem where, the injectivity constraints are slackened [10].

### 3. AMBER: A SPARQL QUERYING ENGINE

Now we present an overview of our proposal AMBER (Attributed Multigraph Based Engine for RDF querying). AMBER encompasses two different stages: an offline stage during which, RDF data is transformed into multigraph  $G$  and then a set of index structures  $\mathcal{I}$  is constructed that captures the necessary information contained in  $G$ ; an online step during which, a given SPARQL query is transformed into a multigraph  $Q$ , and then by exploiting the subgraph matching techniques along with the already built index structures  $\mathcal{I}$ , the homomorphic matches of  $Q$  in  $G$  are obtained.

Given a multigraph representation  $Q$  of a SPARQL query, AMBER decomposes the query vertices  $U$  into a set of core vertices  $U_c$  and satellite vertices  $U_s$ . Intuitively, a vertex  $u \in U$  is a core vertex, if the degree of the vertex is more than one; on the other hand, a vertex  $u$  with degree one is a satellite vertex. For example, in Figure 2c,  $U_c = \{u_1, u_3, u_5\}$  and  $U_s = \{u_0, u_2, u_4, u_6\}$ . Once decomposed, we run the sub-multigraph matching procedure on the query structure spanned only by the core vertices. However, during the procedure, we also process the satellite vertices (if available) that are connected to a core vertex that is being processed. For example, while processing the core vertex  $u_1$ , we also process the set of satellite vertices  $\{u_0, u_2, u_4\}$  connected to it; whereas, the core vertex  $u_5$  has no satellite vertices to be processed. In this way, as the matching proceeds, the entire structure of the query multigraph  $Q$  is processed to

find the homomorphic embeddings in  $G$ . The set of indexing structures  $\mathcal{I}$  are extensively used during the process of sub-multigraph matching. The homomorphic embeddings are finally translated back to the RDF entities using the inverse mapping function  $\mathcal{M}_v^{-1}$  as discussed in Section 2.

## 4. INDEX CONSTRUCTION

Given a data multigraph  $G$ , we build the following three different indices: (i) an inverted list  $\mathcal{A}$  for storing the set of data vertex for each attribute in  $A$  (ii) a trie index structure  $\mathcal{S}$  to store features of all the data vertices  $V$  (iii) a set of trie index structures  $\mathcal{N}$  to store the neighbourhood information of each data vertex  $v \in V$ . For brevity of representation, we ensemble all the three index structures into  $\mathcal{I} := \{\mathcal{A}, \mathcal{S}, \mathcal{N}\}$ .

During the query matching procedure (the online step), we access these indexing structures to obtain the candidate solutions for a query vertex  $u$ . Formally, for a query vertex  $u$ , the *candidate solutions* are a set of data vertices  $C_u = \{v | v \in V\}$  obtained by accessing  $\mathcal{A}$  or  $\mathcal{S}$  or  $\mathcal{N}$ , denoted as  $C_u^{\mathcal{A}}$ ,  $C_u^{\mathcal{S}}$  and  $C_u^{\mathcal{N}}$  respectively.

### 4.1 Attribute Index

The set of vertex attributes is given by  $A = \{a_0, \dots, a_n\}$  (Section 2), where a data vertex  $v \in V$  might have a subset of  $A$  assigned to it. We now build the vertex attribute index  $\mathcal{A}$  by creating an inverted list where a particular attribute  $a_i$  has the list of all the data vertices in which it appears.

Given a query vertex  $u$  with a set of vertex attributes  $u.A \subseteq A$ , for each attribute  $a_i \in u.A$ , we access the index structure  $\mathcal{A}$  to fetch a set of data vertices that have  $a_i$ . Then we find a common set of data vertices that have the entire attribute set  $u.A$ . For example, considering the query vertex  $u_5$  (Fig. 2c), it has an attribute set  $\{a_1, a_2\}$ . The candidate solutions for  $u_5$  are obtained by finding all the common data vertices, in  $\mathcal{A}$ , between  $a_1$  and  $a_2$ , resulting in  $C_{u_5}^{\mathcal{A}} = \{v_0\}$ .

### 4.2 Vertex Signature Index

The index  $\mathcal{S}$  captures the edge type information from the data vertices. For a lucid understanding of this indexing schema we formally introduce the notion of vertex signature that is defined for a vertex  $v \in V$ , which encapsulates the edge information associated with it.

Data vertex	Signature	Synopsis							
		$f_1^+$	$f_2^+$	$f_3^+$	$f_4^+$	$f_1^-$	$f_2^-$	$f_3^-$	$f_4^-$
$v$	$\sigma_v$								
$v_0$	$\{\{-t_6\}, \{t_7\}\}$	1	1	-7	7	1	1	-6	6
$v_1$	$\{\{-t_3\}, \{-t_7\}, \{-t_8\}, \{-t_4, -t_5\}\}$	0	0	0	0	2	5	-3	8
$v_2$	$\{\{-t_0\}, \{t_1\}, \{-t_2\}, \{t_5\}, \{t_6\}, \{t_4, t_5\}\}$	2	4	-1	6	1	2	0	2
$v_3$	$\{\{t_0\}, \{t_3\}, \{-t_1\}\}$	1	2	0	3	1	1	-1	1
$v_4$	$\{\{t_2\}\}$	1	1	-2	2	0	0	0	0
$v_5$	$\{\{t_3\}, \{t_3\}\}$	1	1	-3	3	0	0	0	0
$v_6$	$\{\{t_8\}, \{-t_3\}\}$	1	1	-8	8	1	1	-3	3
$v_7$	$\{\{-t_0\}, \{-t_3\}, \{-t_5\}\}$	0	0	0	0	1	3	0	5
$v_8$	$\{\{t_0\}\}$	1	1	0	0	0	0	0	0

Table 3: Vertex signatures and the corresponding synopses for the vertices in the data multigraph  $G$  (Figure 1c)

DEFINITION 3. Vertex signature. For a vertex  $v \in V$ , the vertex signature  $\sigma_v$  is a multiset containing all the directed multi-edges that are incident on  $v$ , where a multi-edge between  $v$  and a neighbouring vertex  $v'$  is represented by a set that corresponds to the edge types. Formally,  $\sigma_v = \bigcup_{v' \in N(v)} L_E(v, v')$  where  $N(v)$  is the set of neighbourhood vertices of  $v$ , and  $\cup$  is the union operator for multiset.

The index  $\mathcal{S}$  is constructed by tailoring the information supplied by the vertex signature of each vertex in  $G$ . To extract some interesting features, let us observe the vertex signature  $\sigma_{v_2}$  as supplied in Table 3. To begin with, we can represent the vertex signature  $\sigma_{v_2}$  separately for the incoming and outgoing multi-edges as  $\sigma_{v_2}^+ = \{\{t_1\}, \{t_5\}, \{t_6\}, \{t_4, t_5\}\}$  and  $\sigma_{v_2}^- = \{\{-t_0\}, \{-t_2\}\}$  respectively. Now we observe that  $\sigma_{v_2}^+$  has four distinct multi-edges and  $\sigma_{v_2}^-$  has two distinct multi-edges. Now, lets think that we want find candidate solutions for a query vertex  $u$ . The data vertex  $v_2$  can be a match for  $u$  only if the signature of  $u$  has at most four incoming ('+') edges and at most two outgoing ('-') edges; else  $v_2$  can not be a match for  $u$ . Thus, more such features (e.g., maximum cardinality of a set in the vertex signature) can be proposed to filter out irrelevant candidate vertices. Thus, for each vertex  $v$ , we propose to extract a set of features by exploiting the corresponding vertex signature. These features constitute a *synopses*, which is a surrogate representation that approximately captures the vertex signature information.

The synopsis of a vertex  $v$  contains a set of features  $F$ , whose values are computed from the vertex signature  $\sigma_v$ . In this background, we propose four distinct features:  $f_1$  - the maximum cardinality of a set in the vertex signature;  $f_2$  - the number of unique dimensions in the vertex signature;  $f_3$  - the minimum index value of the edge type;  $f_4$  - the maximum index value of the edge type. For  $f_3$  and  $f_4$ , the index values of edge type are nothing but the position of the sequenced alphabet. These four basic features are replicated separately for outgoing (negative) and incoming (positive) edges, as seen in Table 3. Thus for the vertex  $v_2$ , we obtain  $f_1^+ = 2$ ,  $f_2^+ = 4$ ,  $f_3^+ = -1$  and  $f_4^+ = 7$  for the incoming edge set and  $f_1^- = 1$ ,  $f_2^- = 2$ ,  $f_3^- = 0$  and  $f_4^- = 2$  for the outgoing edge set. Synopses for the entire vertex set  $V$  for the data multigraph  $G$  are depicted in Table 3.

Once the synopses are computed for all data vertices, an R-tree is constructed to store all the synopses. This R-tree constitutes the vertex signature index  $\mathcal{S}$ . A synopsis with  $|F|$  fields forms a leaf in the R-tree.

When a set of possible candidate solutions are to be obtained for a query vertex  $u$ , we create a vertex signature  $\sigma_u$  in

order to compute the synopsis, and then obtain the possible solutions from the R-tree structure.

The general idea of using an R-tree is as follows. A synopsis  $F$  of a data vertex spans an axes-parallel rectangle in an  $|F|$ -dimensional space, where the maximum co-ordinates of the rectangle are the values of the synopses fields ( $f_1, \dots, f_{|F|}$ ), and the minimum co-ordinates are the origin of the rectangle (filled with zero values). For example, a data vertex represented by a synopsis with two features  $F(v) = [2, 3]$  spans a rectangle in a 2-dimensional space in the interval range  $([0, 2], [0, 3])$ . Now, if we consider synopses of two query vertices,  $F(u_1) = [1, 3]$  and  $F(u_2) = [1, 4]$ , we observe that the rectangle spanned by  $F(u_1)$  is wholly contained in the rectangle spanned by  $F(v)$  but  $F(u_2)$  is not wholly contained in  $F(v)$ . Thus,  $u_1$  is a candidate match while  $u_2$  is not.

LEMMA 1. Querying the vertex signature index  $\mathcal{S}$  constructed with synopses, guarantees to output at least the entire set of candidate solutions.

PROOF. Consider the field  $f_1^\pm$  in the synopses that represents the maximum cardinality of the neighbourhood signature. Let  $\sigma_u$  be the signature of the query vertex  $u$  and  $\{\sigma_{v_1}, \dots, \sigma_{v_n}\}$  be the set of signatures on the data vertices. By using  $f_1$  we need to show that  $C_u^S$  has at least all the valid candidate matches. Since we are looking for a superset of query vertex signature, and we are checking the condition  $f_1^\pm(u) \leq f_1^\pm(v_i)$ , where  $v_i \in V$ , a vertex  $v_i$  is pruned if it does not match the inequality criterion since, it can never be an eligible candidate. This analogy can be extended to the entire synopses, since it can be applied disjunctively.  $\square$

Formally, the candidates solutions for a vertex  $u$  can be written as  $C_u^S = \{v | \forall_{i \in [1, \dots, |F|]} f_i^\pm(u) \leq f_i^\pm(v)\}$ , where the constraints are met for all the  $|F|$ -dimensions. Since we apply the same inequality constraint to all the fields, we negate the fields that refer to the minimal index value of the edge type ( $f_3^+$  and  $f_3^-$ ) so that the rectangular containment problem still holds good. Further to respect the rectangular containment, we populate the synopses fields with '0' values, in case, the signature does not have either positive or negative edges in it, as seen for  $v_1, v_3, v_4, v_5$  and  $v_7$ .

For example, if we want to compute the possible candidates for a query vertex  $u_0$  in Figure 2c, whose signature is  $\sigma_{u_0} = \{-t_5\}$ , we compute the synopsis which is  $[0 \ 0 \ 0 \ 0 \ 1 \ 1 \ 5 \ 5]$ . Now we look for all those vertices that subsume this synopsis

in the R-tree, whose elements are depicted in Table 3, which gives us the candidate solutions  $C_{u_0}^S = \{v_1, v_7\}$ , thus pruning the rest of the vertices.

The  $S$  index helps to prune the vertices that do not respect the edge type constraints. This is crucial since this pruning is performed for the initial query vertex, and hence many candidates are cast away, thereby avoiding unnecessary recursion during the matching procedure. For example, for the initial query vertex  $u_0$ , whose candidate solutions are  $\{v_1, v_7\}$ , the recursion branch is run only on these two starting vertices instead of the entire vertex set  $V$ .

### 4.3 Vertex Neighbourhood Index

The *vertex neighbourhood index*  $\mathcal{N}$  captures the topological structure of the data multigraph  $G$ . The index  $\mathcal{N}$  comprises of 1-neighbourhood trees built for each data vertex  $v \in V$ . Since  $G$  is a directed multigraph, and each vertex  $v \in V$  can have both the incoming and outgoing edges, we construct two separate index structures  $\mathcal{N}^+$  and  $\mathcal{N}^-$  for incoming and outgoing edges respectively, that constitute the structure  $\mathcal{N}$ .

To understand the index structure, let us consider the data vertex  $v_2$  from Figure 1c, shown separately in Figure 3a. For this vertex  $v_2$ , we collect all the neighbourhood information (vertices and multi-edges), and represent this information by a tree structure, built separately for incoming ('+') and outgoing ('-') edges. Thus, the tree representation of a vertex  $v$  contains the neighbourhood vertices and the corresponding multi-edges, as shown in Figure 3b, where the vertices of the tree structure are represented by the edge types.

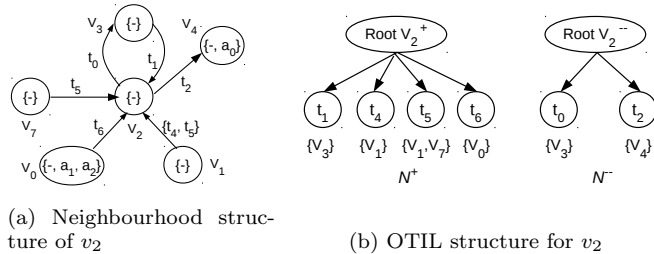
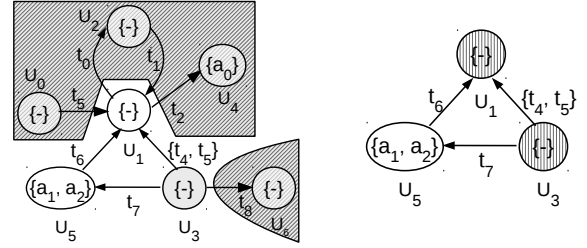


Figure 3: Building Neighbourhood Index for data vertex  $v_2$

In order to construct an efficient tree structure, we take inspiration from [13] to propose the structure - Ordered Trie with Inverted List (OTIL). To construct the OTIL index as shown in Figure 3b, we insert each ordered multi-edge that is incident on  $v$  at the root of the trie. Consider a data vertex  $v_i$ , with a set of  $n$  neighbourhood vertices  $N(v_i)$ . Now, for every pair of incoming edge  $(v_i, N^j(v_i))$ , where  $j \in \{1, \dots, n\}$ , there exists a multi-edge  $\{t_i, \dots, t_j\}$ , which is inserted into the OTIL structure  $\mathcal{N}^+$ . Similarly for every pair of outgoing edge  $(N^j(v_i), v_i)$ , there exists a multi-edge  $\{t_m, \dots, t_n\}$ , which is inserted into the OTIL structure  $\mathcal{N}^-$  maintaining two OTIL structures that constitute  $\mathcal{N}$ . Each multi-edge is ordered (w.r.t. increasing edge type indexes), before inserting into the respective OTIL structure, and the order is universally maintained for all data vertices. Further, for every edge type  $t_i$ , we maintain a *list* that contains all the neighbourhood vertices  $N^+(v_i)/N^-(v_i)$ , that have the edge type  $t_i$  incident on them.



(a) Query graph  $Q$  highlighted with satellite vertices (b) Query graph spanned by core vertices

Figure 4: Decomposing the query multigraph into *core* and *satellite* vertices

To understand the utility of  $\mathcal{N}$ , let us consider an illustrative example. Considering the query multigraph  $Q$  in Figure 2c, let us assume that we want to find the matches for the query vertices  $u_1$  and  $u_0$  in order. Thus, for the initial vertex  $u_1$ , let us say, we have found the set of candidate solutions which is  $\{v_2\}$ . Now, to find the candidate solutions for the next query vertex  $u_0$ , it is important to maintain the structure spanned by the query vertices, and this is where the indexing structure  $\mathcal{N}$  is accessed. Thus to retain the structure of the query multigraph (in this case, the structure between  $u_1$  and  $u_0$ ), we have to find the data vertices that are in the neighbourhood of already matched vertex  $v_2$  (a match for vertex  $u_1$ ), that has the same structure (edge types) between  $u_1$  and  $u_0$  in the query graph. Thus to fetch all the data vertices that have the edge type  $t_5$ , which is directed towards  $v_2$  and hence '+', we access the neighbourhood index trie  $\mathcal{N}^+$  for vertex  $v_2$ , as shown in Figure 3. This gives us a set of candidate solutions  $C_{u_0}^{\mathcal{N}} = \{v_1, v_7\}$ . It is easy to observe that, by maintaining two separate indexing structures  $\mathcal{N}^+$  and  $\mathcal{N}^-$ , for both incoming and outgoing edges, we can reduce the time to fetch the candidate solutions.

Thus, in a generic scenario, given an already matched data vertex  $v$ , the edge direction '+' or '-', and the set of edge types  $T' \subseteq T$ , the index  $\mathcal{N}$  will find a set of neighbourhood data vertices  $\{v' | (v', v) \in E \wedge T' \subseteq L_E(v', v)\}$  if the edge direction is '+' (incoming), while  $\mathcal{N}$  returns  $\{v' | (v, v') \in E \wedge T' \subseteq L_E(v, v')\}$  if the edge direction is '-' (outgoing).

## 5. QUERY MATCHING PROCEDURE

In order to follow the working of the proposed query matching procedure, we formalize the notion of *core* and *satellite* vertices. Given a query graph  $Q$ , we decompose the set of query vertices  $U$  into a set of *core* vertices  $U_c$  and a set of *satellite* vertices  $U_s$ . Formally, when the degree of the query graph  $\Delta(Q) > 1$ ,  $U_c = \{u | u \in U \wedge deg(u) > 1\}$ ; however, when  $\Delta(Q) = 1$ , i.e., when the query graph is either a vertex or a multiedge, we choose one query vertex at random as a *core* vertex, and hence  $|U_c| = 1$ . The remaining vertices are classified as satellite vertices, whose degree is always 1. Formally,  $U_s = \{U \setminus U_c\}$ , where for every  $u \in U_s$ ,  $deg(u) = 1$ . The decomposition for the query multigraph  $Q$  is depicted in Figure 4, where the satellite vertices are separated (vertices under the shaded region in Fig. 4a), in order to obtain the query graph that is spanned only by the core vertices (Fig. 4b).

The proposed AMBER-Algo (Algorithm 3) performs recursive sub-multigraph matching procedure only on the query structure spanned by  $U_c$  as seen in Figure 4b. Since the entire set of satellite vertices  $U_s$  is connected to the query structure spanned by the core vertices, AMBER-Algo processes the satellite vertices while performing sub-multigraph matching on the set of core vertices. Thus during the recursion, if the current *core* vertex has *satellite* vertices connected to it, the algorithm retrieves directly a list of possible matching for such *satellite* vertices and it includes them in the current partial solution. Each time the algorithm executes a recursion branch with a solution, the solution not only contains a data vertex match  $v_c$  for each query vertex belonging to  $U_c$ , but also a set of matched data vertices  $V_s$  for each query vertex belonging to  $U_s$ . Each time a solution is found, we can generate not only one, but a set of embeddings through the Cartesian product of the matched elements in the solution.

Since finding SPARQL solutions is equivalent to finding homomorphic embeddings of the query multigraph, the homomorphic matching allows different query vertices to be matched with the same data vertices. Recall that there is no injectivity constraint in sub-multigraph homomorphism as opposed to sub-multigraph isomorphism [10]. Thus during the recursive matching procedure, we do not have to check if the potential data vertex has already been matched with previously matched query vertices. This is an advantage when we are processing satellite vertices: we can find matches for each satellite vertex independently without the necessity to check for a repeated data vertex.

Before getting into the details of the AMBER-Algo, we first explain how a set of candidate solutions is obtained when there is information associated only with the vertices. Then we explain how a set of candidate solutions is obtained when we encounter the satellite vertices.

## 5.1 Vertex Level Processing

To understand the generic query processing, it is necessary to understand the matching process at vertex level. Whenever a query vertex  $u \in U$  is being processed, we need to check if  $u$  has a set of attributes  $A$  associated with it or any *IRIs* are connected to it (recall Section 2.2).

---

### Algorithm 1: PROCESSVERTEX( $u, Q, \mathcal{A}, \mathcal{N}$ )

---

```

1 if  $u.A \neq \emptyset$  then
2    $C_u^A = \text{QUERYATTINDEX}(\mathcal{A}, u.A)$ 
3 if  $u.R \neq \emptyset$  then
4    $C_u^I = \bigcap_{u_i^{iri} \in u.R} (\text{QUERYNEIGHINDEX}(\mathcal{N}, L_E^Q(u, u_i^{iri}), u_i^{iri}))$ 
5  $CandAtt_u = C_u^A \bar{\cap} C_u^I$  /* Find common candidates */
6 return  $CandAtt_u$ 

```

---

To process an arbitrary query vertex, we propose a procedure PROCESSVERTEX, depicted in Algorithm 1. This algorithm is invoked only when a vertex  $u$  has at least, either a set of vertex attributes or any *IRI* associated with it. The PROCESSVERTEX procedure returns a set of data vertices  $CandAtt_u$ , which are matchable with  $u$ ; in case  $CandAtt_u$  is empty, then the query vertex  $u$  has no matches in  $V$ .

As seen in Lines 1-2, when a query vertex  $u$  has a set of

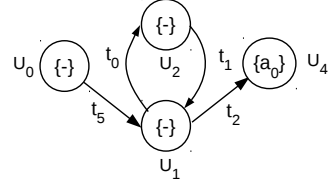


Figure 5: A star structure in the query multigraph  $Q$

vertex attributes i.e.,  $u.A \neq \emptyset$ , we obtain the candidate solutions  $C_u^A$  by invoking QUERYATTINDEX procedure, that accesses the index  $\mathcal{A}$  as explained in Section 4.1. For example, the query vertex  $u_5$  with vertex attributes  $\{a_1, a_2\}$ , can only be matched with the data vertex  $v_0$ ; thus  $C_{u_5}^A = \{v_0\}$ .

When a query vertex  $u$  has *IRIs* associated with it, i.e.,  $u.R \neq \emptyset$  (Lines 3-4), we find the candidate solutions  $C_u^I$  by invoking the QUERYNEIGHINDEX procedure. As we recall from Section 2.2, a vertex  $u$  is connected to an *IRI* vertex  $u_i^{iri}$  through a multi-edge  $L_E^Q(u, u_i^{iri})$ . An *IRI* vertex  $u_i^{iri}$  always has only one data vertex  $v$ , that can match. Thus, the candidate solutions  $C_u^I$  are obtained by invoking the QUERYNEIGHINDEX procedure, that fetches all the neighbourhood vertices of  $v$  that respect the multi-edge  $L_E^Q(u, u_i^{iri})$ . The procedure is invoked until all the *IRI* vertices  $u.R$  are processed (Line 4). Considering the example in Figure 2c,  $u_3$  is connected to an *IRI*-vertex  $u_0^{iri}$ , which has a unique data vertex match  $v_5$ , through the multi-edge  $\{-t_3\}$ . Using the neighbourhood index  $\mathcal{N}$ , we look for the neighbourhood vertices of  $v_5$ , that have the multi-edge  $\{-t_3\}$ , which gives us the candidate solutions  $C_{u_3}^I = \{v_1\}$ .

Finally in Line 5, the merge operator  $\bar{\cap}$  returns a set of common candidates  $CandAtt_u$ , only if  $u.A \neq \emptyset$  and  $u.R \neq \emptyset$ . Otherwise,  $C_u^A$  or  $C_u^I$  are returned as  $CandAtt_u$ .

## 5.2 Processing Satellite Vertices

In this section, we provide insights on processing a set of satellite vertices  $U_{sat} \subseteq U_s$  that are connected to a core vertex  $u_c \in U_c$ . This scenario results in a structure that appears frequently in SPARQL queries called star structure [7, 9].

A typical star structure depicted in Figure 5, has a core vertex  $u_c = u_1$ , and a set of satellite vertices  $U_{sat} = \{u_0, u_2, u_4\}$  connected to the core vertex. For each candidate solution of the core vertex  $u_1$ , we process  $u_0, u_2, u_4$  independently of each other, since there is no structural connectivity (edges) among them, although they are only structurally connected to the core vertex  $u_1$ .

LEMMA 2. *For a given star structure in a query graph, each satellite vertex can be independently processed if a candidate solution is provided for the core vertex  $u_c$ .*

PROOF. Consider a core vertex  $u_c$  that is connected to a set of satellite vertices  $U_{sat} = \{u_0, \dots, u_s\}$ , through a set of edge-types  $T' = \{t_0, \dots, t_s\}$ . Let us assume  $v_c$  is a candidate solution for the core vertex  $u_c$ , and we want to find candidate solutions for  $u_i \in U_{sat}$  and  $u_j \in U_{sat}$ ,



where  $i \neq j$ . Now, the candidate solutions for  $u_i$  and  $u_j$  can be obtained by fetching the neighbourhoods of already matched vertex  $v_c$  that respect the edge-type  $t_i \in T'$  and  $t_j \in T'$  respectively. Since two satellite vertices  $u_i$  and  $u_j$  are never connected to each other, the candidate solutions of  $u_i$  are independent of that of  $u_j$ . This analogy applies to all the satellite vertices.  $\square$

---

**Algorithm 2:** MATCHSATVERTICES( $\mathcal{A}, \mathcal{N}, Q, U_{sat}, v_c$ )

---

```

1 SET:  $M_{sat} = \emptyset$ , where  $M_{sat} = \{[u_s, V_s]\}_{s=1}^{|U_{sat}|}$ 
2 for all  $u_s \in U_{sat}$  do
3    $Cand_{u_s} = \text{QUERYNEIGHINDEX}(\mathcal{N}, L_E^Q(u_c, u_s), v_c)$ 
4    $Cand_{u_s} = Cand_{u_s} \cap \text{PROCESSVERTEX}(u_s, Q, \mathcal{A}, \mathcal{N})$ 
5   if  $Cand_{u_s} \neq \emptyset$  then
6      $M_{sat} = M_{sat} \cup (u_s, Cand_{u_s})$  /* Satellite solutions */
7   else
8     return  $M_{sat} := \emptyset$  /* No solutions possible */
9 return  $M_{sat}$  /* Matches for satellite vertices */
```

---

Given a core vertex  $u_c$ , we initially find a set of candidate solutions  $Cand_{u_c}$ , by using the index  $\mathcal{S}$ . Then, for each candidate solution  $v_c \in Cand_{u_c}$ , the set of solutions for all the satellite vertices  $U_{sat}$  that are connected to  $u_c$  are returned by the MATCHSATVERTICES procedure, described in Algorithm 2. The set of solution tuple  $M_{sat}$  defined in Line 1, stores the candidate solutions for the entire set of satellite vertices  $U_{sat}$ . Formally,  $M_{sat} = \{[u_s, V_s]\}_{s=1}^{|U_{sat}|}$ , where  $u_s \in U_{sat}$  and  $V_s$  is a set of candidate solutions for  $u_s$ . In order to obtain candidate solutions for  $u_s$ , we query the neighbourhood index  $\mathcal{N}$  (Line 3); the QUERYNEIGHINDEX function obtains all the neighbourhood vertices of already matched  $v_c$ , that also considers the multi-edge in the query multigraph  $L_E^Q(u_c, u_s)$ . As every query vertex  $u_s \in U_{sat}$  is processed, the solution set  $M_{sat}$  that contains candidate solutions grows until all the satellite vertices have been processed (Lines 2-8).

In Line 4, the set of candidate solutions  $Cand_{u_s}$  are refined by invoking Algorithm 1 (VERTEXPROCESSING). After the refinement, if there are finite candidate solutions, we update the solution  $M_{sat}$ ; else, we terminate the procedure as there can be no matches for a given matched vertex  $v_c$ . The MATCHSATVERTICES procedure performs two tasks: firstly, it checks if the candidate vertex  $v_c \in Cand_{u_s}$  is a valid matchable vertex and secondly, it obtains the solutions for all the satellite vertices.

### 5.3 Arbitrary Query Processing

Algorithm 3 shows the generic procedure we develop to process arbitrary queries.

Recall that for an arbitrary query  $Q$ , we define two different types of vertexes: a set of core vertices  $U_c$  and a set of satellite vertices  $U_s$ . The QUERYDECOMPOSE procedure in Line 1 of Algorithm 3, performs this decomposition by splitting the query vertices  $U$  into  $U_c$  and  $U_s$ , as observed in Figure 4.

To process arbitrary query multigraphs, we perform recursive sub-multigraph matching procedure on the set of core vertices  $U_c \subseteq U$ ; during the recursion, satellite vertexes connected to a specific core vertex are processed too. Since the

recursion is performed on the set of core vertices, we propose a few heuristics for ordering the query vertexes.

Ordering of the query vertexes forms one of the vital steps for subgraph matching algorithms [10]. In any subgraph matching algorithm, the embeddings of a query subgraph are obtained by exploring the solution space spanned by the data graph. But since the solution space itself can grow exponentially in size, we are compelled to use intelligent strategies to traverse the solution space. In order to achieve this, we propose a heuristic procedure VERTEXORDERING (Line 2, Algorithm 3) that employs two ranking functions.

The first ranking function  $r_1$  relies on the number of satellite vertexes connected to the core vertex, and the query vertexes are ordered with the decreasing rank value. Formally,  $r_1(u) = |U_{sat}|$ , where  $U_{sat} = \{u_s | u_s \in U_s \wedge (u, u_s) \in E(Q)\}$ . A vertex with more satellite vertexes connected to it, is rich in structure and hence it would probably yield fewer candidate solutions to be processed under recursion. Thus, in Figure 4,  $u_1$  is chosen as an initial vertex. The second ranking function  $r_2$  relies on the number of incident edges on a query vertex. Formally,  $r_2(u) = \sum_{j=1}^m |\sigma(u)^j|$ , where  $u$  has  $m$  multiedges and  $|\sigma(u)^j|$  captures the number of edge types in the  $j^{\text{th}}$  multiedge. Again,  $U_c^{ord}$  contains the ordered vertexes with the decreasing rank value  $r_2$ . Further, when there are no satellite vertexes in the query  $Q$ , this ranking function gets the priority. Despite the usage of any ranking function, the query vertexes in  $U_c^{ord}$ , when accessed in sequence, should be structurally connected to the previous set of vertexes. If two vertexes tie up with the same rank, the rank with lesser priority determines which vertex wins. Thus, for the example in Figure 4, the set of ordered core vertexes is  $U_c^{ord} = \{u_1, u_3, u_5\}$ .

---

**Algorithm 3:** AMBER-Algo ( $\mathcal{I}, Q$ )

---

```

1 QUERYDECOMPOSE: Split  $U$  into  $U_c$  and  $U_s$ 
2  $U_c^{ord} = \text{VERTEXORDERING}(Q, U_c)$ 
3  $u_{init} = u | u \in U_c^{ord}$ 
4  $CandInit = \text{QUERYSYNINDEX}(u_{init}, \mathcal{S})$ 
5  $CandInit = CandInit \cap \text{PROCESSVERTEX}(u_{init}, Q, \mathcal{A}, \mathcal{N})$ 
6 FETCH:  $U_{init}^{sat} = \{u | u \in U_s \wedge (u_{init}, u) \in E(Q)\}$ 
7 SET:  $Emb = \emptyset$ 
8 for  $v_{init} \in CandInit$  do
9   SET:  $M = \emptyset, M_s = \emptyset, M_c = \emptyset$ 
10  if  $U_{init}^{sat} \neq \emptyset$  then
11     $M_{sat} = \text{MATCHSATVERTICES}(\mathcal{A}, \mathcal{N}, Q, U_{init}^{sat}, v_{init})$ 
12    if  $M_{sat} \neq \emptyset$  then
13      for  $[u_s, V_s] \in M_{sat}$  do
14        UPDATE:  $M_s = M_s \cup [u_s, V_s]$ 
15        UPDATE:  $M_c = M_c \cup [u_{init}, v_{init}]$ 
16         $Emb = Emb \cup \text{HOMOMORPHICMATCH}(M, \mathcal{I}, Q, U_c^{ord})$ 
17  else
18    UPDATE:  $M_c = M_c \cup (u_{init}, v_{init})$ 
19     $Emb = Emb \cup \text{HOMOMORPHICMATCH}(M, \mathcal{I}, Q, U_c^{ord})$ 
20 return  $Emb$  /* Homomorphic embeddings of query multigraph */
```

---

The first vertex in the set  $U_c^{ord}$  is chosen as the initial vertex  $u_{init}$  (Line 3), and subsequent query vertexes are chosen in sequence. The candidate solutions for the initial query vertex  $CandInit$  are returned by QUERYSYNINDEX procedure (Line 4), that are constrained by the structural properties (neighbourhood structure) of  $u_{init}$ . By querying the index  $\mathcal{S}$  for initial query vertex  $u_{init}$ , we obtain the candidate so-

lutions  $CandInit \in V$  that match the structure (multi-edge types) associated with  $u_{init}$ . Although some candidates in  $CandInit$  may be invalid, all valid candidates are present in  $CandInit$ , as deduced in Lemma 1. Further, PROCESSVERTEX procedure is invoked to obtain the candidates solutions according to vertex attributes and IRI information, and then only the common candidates are retained.

Before getting into the details of the algorithm, we explain how the solutions are handled and how we process each query vertex. We define  $M$  as a set of tuples, whose  $i^{th}$  tuple is represented as  $M_i = [m_c, M_s]$ , where  $m_c$  is a solution pair for a core vertex, and  $M_s$  is a set of solution pairs for the set of satellite vertices that are connected to the core vertex. Formally,  $m_c = (u_c, v_c)$ , where  $u_c$  is the core vertex and  $v_c$  is the corresponding matched vertex;  $M_s$  is a set of solution pairs, whose  $j^{th}$  element is a solution pair  $(u_s, V_s)$ , where  $u_s$  is a satellite vertex and  $V_s$  is a set of matched vertices. In addition, we maintain a set  $M_c$  whose elements are the solution pairs for all the core vertices. Thus during each recursion branch, the size of  $M$  grows until it reaches the query size  $|U|$ ; once  $|M| = |U|$ , homomorphic matches are obtained.

For all the candidate solutions of initial vertex  $CandInit$ , we perform recursion to obtain homomorphic embeddings (lines 8-19). Before getting into recursion, for each initial match  $v_{init} \in CandInit$ , if it has satellite vertices connected to it, we invoke the MATCHSATVERTICES procedure (Lines 10-11). This step not only finds solution matches for satellite vertices, if there are, but also checks if  $v_{init}$  is a valid candidate vertex. If the returned solution set  $M_{sat}$  is empty, then  $v_{init}$  is not a valid candidate and hence we continue with the next  $v_{init} \in CandInit$ ; else, we update the set of solution pairs  $M_s$  for satellite vertices and the solution pair  $M_c$  for the core vertex (Lines 12-15) and invoke HOMOMORPHICMATCH procedure (Lines 17). On the other hand, if there are no satellite vertices connected to  $u_{init}$ , we update the core vertex solution set  $M_c$  and invoke HOMOMORPHICMATCH procedure (Lines 18-19).

---

**Algorithm 4:** HOMOMORPHICMATCH( $M, \mathcal{I}, Q, U_c^{ord}$ )

---

```

1 if  $|M| = |U|$  then
2   return GENEMB( $M$ )
3  $Emb = \emptyset$ 
4 FETCH:  $u_{next} = u | u \in U_c^{ord}$ 
5  $N_q = \{u_c | u_c \in M_c\} \cap adj(u_{next})$ 
6  $N_g = \{v_c | v_c \in M_c \wedge (u_c, v_c) \in M_c\}$ , where  $u_c \in N_q$ 
7  $Cand_{u_{next}} = \bigcap_{n=1}^{|N_q|} (\text{QueryNeighIndex}(\mathcal{N}, L_E^Q(u_n, u_{next}), v_n))$ 
8  $Cand_{u_{next}} = Cand_{u_{next}} \cap \text{PROCESSVERTEX}(u_{next}, Q, \mathcal{A}, \mathcal{N})$ 
9 for each  $v_{next} \in Cand_{u_{next}}$  do
10  FETCH:  $U_{next}^{sat} = \{u | u \in V_s \wedge (u_{next}, u) \in E(Q)\}$ 
11  if  $U_{next}^{sat} \neq \emptyset$  then
12     $M_{sat} = \text{MATCHSATVERTICES}(\mathcal{A}, \mathcal{N}, Q, U_{next}^{sat}, v_{next})$ 
13    if  $M_{sat} \neq \emptyset$  then
14      for every  $[u^s, V^s] \in M_{sat}$  do
15        UPDATE:  $M_s = M_s \cup [u^s, V^s]$ 
16      UPDATE:  $M_c = M_c \cup (u_{next}, v_{next})$ 
17       $Emb = Emb \cup \text{HOMOMORPHICMATCH}(M, \mathcal{I}, Q, U_c^{ord})$ 
18  else
19    UPDATE:  $M_c = M_c \cup (u_{next}, v_{next})$ 
20     $Emb = Emb \cup \text{HOMOMORPHICMATCH}(M, \mathcal{I}, Q, U_c^{ord})$ 
21 return  $Emb$ 

```

---

In the HOMOMORPHICMATCH procedure (Algorithm 4), we fetch the next query vertex from the set of ordered core vertices  $U_c^{ord}$  (Line 4). Then we collect the neighbourhood vertices of already matched core query vertices and the corresponding matched data vertices (Lines 5-6). As we recall, the set  $M_c$  maintains the solution pair  $m_c = (u_c, v_c)$  of each matched core query vertex. The set  $N_q$  collects the already matched core vertices  $u_c \in M_c$  that are also in the neighbourhood of  $u_{next}$ , whose matches have to be found. Further,  $N_g$  contains the corresponding matched query vertices  $v_c \in M_c$ . As the recursion proceeds further, we can find only those matchable data vertices of  $u_{next}$  that are in the neighbourhood of all the matched vertices  $v \in N_g$ , so that the query structure is maintained. In Line 7, for each  $u_n \in N_q$  and the corresponding  $v_n \in N_g$ , we query the neighbourhood index  $\mathcal{N}$ , to obtain the candidate solutions  $Cand_{u_{next}}$ , that are in the neighbourhood of already matched data vertex  $v_n$  and have the multi-edge  $L_E^Q(u_n, u_{next})$ , obtained from the query multigraph  $Q$ . Finally (line 7), only the set of candidates solutions that are common for every  $u_n \in N_q$  are retained in  $Cand_{u_{next}}$ .

Further, the candidate solutions are refined with the help of PROCESSVERTEX procedure (Line 8). Now, for each of the valid candidate solution  $v_{next} \in Cand_{u_{next}}$ , we recursively call the HOMOMORPHICMATCH procedure. When the next query vertex  $u_{next}$  has no satellite vertices attached to it, we update the core vertex solution set  $M_c$  and call the recursion procedure (Lines 19-20). But when  $u_{next}$  has satellite vertices attached to it, we obtain the candidate matches for all the satellite vertices by invoking the MATCHSATVERTICES procedure (Lines 11-12); if there are matches, we update both the satellite vertex solution  $M_s$  and the core vertex solution  $M_c$ , and invoke the recursion procedure (Line 17).

Once all the query vertices have been matched for the current recursion step, the solution set  $M$  contains the solutions for both core and satellite vertices. Thus when all the query vertices have been matched, we invoke the GENEMB function (Line 2) which returns the set of embeddings, that are updated in  $Emb$ . The GENEMB function treats the solution vertex  $v_c$  of each core vertex as a singleton and performs Cartesian product among all the core vertex singletons and satellite vertex sets. Formally,  $Emb_{part} = \{v_c^1\} \times \dots \times \{v_c^{|U_c|}\} \times V_s^1 \times \dots \times V_c^{|U_s|}$ . Thus, the partial set of embeddings  $Emb_{part}$  is added to the final result  $Emb$ .

## 6. RELATED WORK

The proliferation of semantic web technologies has influenced the popularity of RDF as a standard to represent and share knowledge bases. In order to efficiently answer SPARQL queries, many stores and API inspired by relational model were proposed [6, 3, 12, 5]. x-RDF-3X [12], inspired by modern RDBMS, represent RDF triples as a big three-attribute table. The RDF query processing is boosted using an exhaustive indexing schema coupled with statistics over the data. Also Virtuoso[6] heavily exploits RDBMS mechanism in order to answer SPARQL queries. Virtuoso is a column-store based systems that employs sorted multi-column column-wise compressed projections. Also these systems build table indexing using standard B-trees. Jena [5] supplies API for manipulating RDF graphs. Jena exploits multiple-property tables that permit multiple views

of graphs and vertices which can be used simultaneously.

Recently, the database community has started to investigate RDF stores based on graph data management techniques [15, 10]. gStore [15] applies graph pattern matching using the filter-and-refinement strategy to answer SPARQL queries. It employs an indexing schema, named VS\*-tree, to concisely represent the RDF graph. Once the index is built, it is used to find promising subgraphs that match the query. Finally, exact subgraphs are enumerated in the refinement step. TurboHom++ [10] is an adaptation of a state of the art subgraph isomorphism algorithm (TurboISO[8]) to the problem of SPARQL queries. Starting from the standard graph isomorphism problem, the authors relax the injectivity constraint in order to handle the graph homomorphism, which is the RDF pattern matching semantics.

Unlike our approach, TurboHom++ does not index the RDF graph, while gStore concisely represents RDF data through VS\*-tree. Another difference between AMBER and the other graph stores is that our approach explicitly manages the multigraph induced by the SPARQL queries while no clear discussion is supplied for the other tools.

## 7. EXPERIMENTAL ANALYSIS

In this section we perform extensive experiments on the three RDF benchmarks. We evaluate the time performance and the robustness of AMBER w.r.t. state-of-the-art competitors by varying the size, and the structure of the SPARQL queries. Experiments are carried out on a 64-bit Intel Core i7-4900MQ @ 2.80GHz, with 32GB memory, running Linux OS - Ubuntu 14.04 LTS. AMBER is implemented in C++.

### 7.1 Experimental Setup

We compare AMBER with the four standard RDF engines: *Virtuoso-7.1* [6], *x-RDF-3X* [12], *Apache Jena* [5] and *gStore* [15]. For all the competitors we employ the source code available on the web site or obtained by the authors. Another recent work *TurboHOM++* [10] has been excluded since it is not publicly available.

For the experimental analysis we use three RDF datasets - *DBPEDIA*, *YAGO* and *LUBM*. *DBPEDIA* constitutes the most important knowledge base for the Semantic Web community. Most of the data available in this dataset comes from the Wikipedia Infobox. *YAGO* is a real world dataset built from factual information coming from *Wikipedia* and *WordNet* semantic network. *LUBM* provides a standard RDF benchmark to test the overall behaviour of engines. Using the data generator we create *LUBM100* where the number represents the scaling factor.

The data characteristics are summarized in Table 4. We can observe that the benchmarks have different characteristics in terms of number of vertices, number of edges, and number of distinct predicates. For instance, *DBPEDIA* has more diversity in terms of predicates (~700) while *LUBM100* contains only 13 different predicates.

The time required to build the multigraph database as well as to construct the indexes are reported in Table 5. We can note that the database building time and the corresponding size are proportional to the number of triples. Regarding

Dataset	# Triples	# Vertices	# Edges	# Edge types
<i>DBPEDIA</i>	33 071 359	4 983 349	14 992 982	676
<i>YAGO</i>	35 543 536	3 160 832	10 683 425	44
<i>LUBM100</i>	13 824 437	2 179 780	8 952 366	13

Table 4: Benchmark Statistics

the indexing structures, we can underline that both building time and size are proportional to the number of edges. For instance, *DBPEDIA* has the biggest number of edges (~15M) and, consequently, AMBER employs more time and space to build and store its data structure.

Dataset	Database		Index $\mathcal{I}$	
	Building Time	Size	Building Time	Size
<i>DBPEDIA</i>	307	1300	45.18	1573
<i>YAGO</i>	379	2400	29.1	1322
<i>LUBM100</i>	67	497	18.4	1057

Table 5: Offline stage: Database and Index Construction time (in seconds) and memory usage (in Mbytes)

### 7.2 Workload Generation

In order to test the scalability and the robustness of the different RDF engines, we generate the query workloads considering a similar setting to [7, 2, 8]. We generate the query workload from the respective RDF datasets, which are available as RDF tripleset. In specific, we generate two types of query sets: a star-shaped and a complex-shaped query set; further, both query sets are generated for varying sizes (say  $k$ ) ranging from 10 to 50 triplets, in steps of 10.

To generate star-shaped or complex-shaped queries of size  $k$ , we pick an initial-entity at random from the RDF data. Now to generate star queries, we check if the initial-entity is present in at least  $k$  triples in the entire benchmark, to verify if the initial-entity has  $k$  neighbours. If so, we choose those  $k$  triples at random; thus the initial entity forms the central vertex of the star structure and the rest of the entities form the remaining star structure, connected by the respective predicates. To generate complex-shaped queries of size  $k$ , we navigate in the neighbourhood of the initial-entity through the predicate links until we reach size  $k$ . In both query types, we inject some object literals as well as constant *IRIs*; rest of the *IRIs* (subjects or objects) are treated as variables. However, this strategy could choose some very unselective queries [7]. In order to address this issue, we set a maximum time constraint of 60 seconds for each query. If the query is not answered in time, it is not considered for the final average (similar procedure is usually employed for graph query matching [8] and RDF workload evaluation [2]). We report the average query time and, also, the percentage of unanswered queries (considering the given time constraint) to study the robustness of the approaches.

### 7.3 Comparison with RDF Engines

In this section we report and discuss the results obtained by the different RDF engines. For each combination of query type and benchmark we report two plots by varying the query size: the average time and the corresponding percentage of unanswered queries for the given time constraint. We

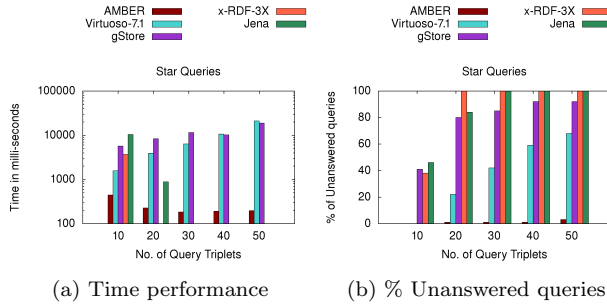


Figure 6: Evaluation of (a) time performance and (b) robustness, for *Star-Shaped* queries on *DBPEDIA*.

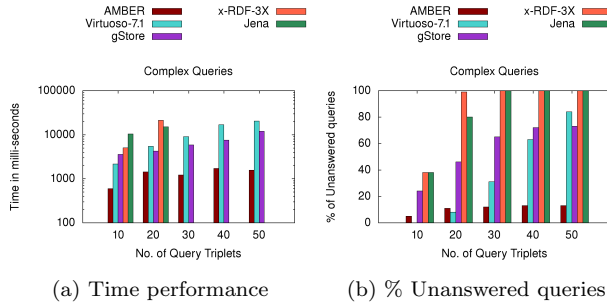


Figure 7: Evaluation of (a) time performance and (b) robustness, for *Complex-Shaped* queries on *DBPEDIA*.

remind that the average time per approach is computed only on the set of queries that were answered.

The experimental results for *DBPEDIA* are depicted in Figure 6 and Figure 7. The time performance (averaged over 200 queries) for *Star-Shaped* queries (Fig. 6a), affirm that AMBER clearly outperforms all the competitors. Further the robustness of each approach, evaluated in terms of percentage of unanswered queries within the stipulated time, is shown in Figure 6b. For the given time constraint, *x-RDF-3X* and *Jena* are unable to output results for size 20 and 30 onwards respectively. Although *Virtuoso* and *gStore* output results until query size 50, their time performance is still poor. However, as the query size increases, the percentage of unanswered queries for both *Virtuoso* and *gStore* keeps on increasing from  $\sim 0\%$  to 65% and  $\sim 45\%$  to 95% respectively. On the other hand AMBER answers  $>98\%$  of the queries, even for queries of size 50, establishing its robustness.

Analyzing the results for *Complex-Shaped* queries (Fig. 7), we underline that AMBER still outperforms all the competitors for all sizes. In Figure 7a, we observe that *x-RDF-3X* and *Jena* are the slowest engines; *Virtuoso* and *gStore* perform better than them but nowhere close to AMBER. We further observe that *x-RDF-3X* and *Jena* are the least robust as they don't output results for size 30 onwards (Fig. 7b); on the other hand AMBER is the most robust engine as it answers  $>85\%$  of the queries even for size 50. The percentage of unanswered queries for *Virtuoso* and *gStore* increase from 0% to  $\sim 80\%$  and 25% to  $\sim 70\%$  respectively, as we increase the size from 10 to 50.

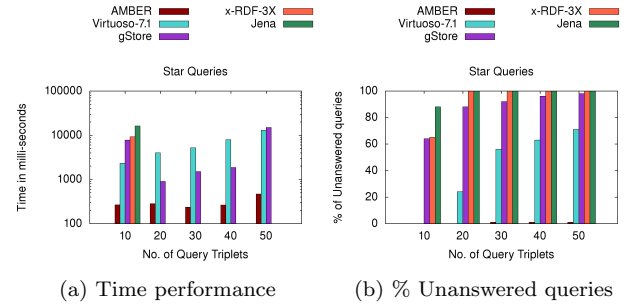


Figure 8: Evaluation of (a) time performance and (b) robustness, for *Star-Shaped* queries on *YAGO*.

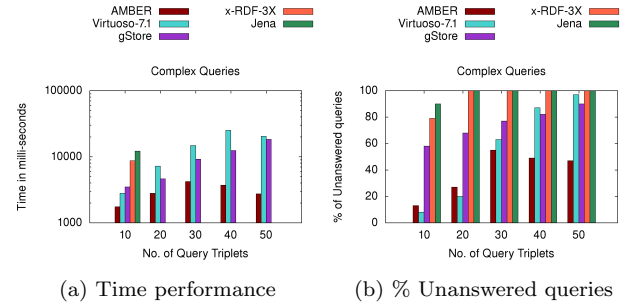


Figure 9: Evaluation of (a) time performance and (b) robustness, for *Complex-Shaped* queries on *YAGO*.

The results for *YAGO* are reported in Figure 8 and Figure 9. For the *Star-Shaped* queries (Fig. 8), we observe that AMBER outperforms all the other competitors for any size. Further, the time performance of AMBER is 1-2 order of magnitude better than its nearest competitor *Virtuoso* (Fig. 8a), and the performance remains stable even with increasing query size (Fig. 8b). *x-RDF-3X*, *Jena* are not able to output results for size 20 onwards. As observed for *DBPEDIA*, *Virtuoso* seems to become less robust with the increasing query size. For size 20-40, time performance of *gStore* seems better than *Virtuoso*; the reason seems to be the fewer queries that are being considered. Conversely, AMBER is able to supply answers most of the time ( $>98\%$ ).

Coming to the results for *Complex-Shaped* queries (Fig. 9), we observe that AMBER is still the best in time performance; *Virtuoso* and *gStore* are the closest competitors. Only for size 10 and 20, *Virtuoso* seems a bit robust than AMBER. *Jena*, *x-RDF-3X* do not answer queries for size 20 onwards, as seen in Figure 9b.

The results for *LUBM100* are reported in Figure 10 and Figure 11. For the *Star-Shaped* queries (Fig. 10), AMBER always outperforms all the other competitors for any size (Fig. 10a). Further, the time performance of AMBER is 2-3 orders of magnitude better than its closest competitor *Virtuoso*. Similar to the *YAGO* experiments, *x-RDF-3X*, *Jena* are not able to manage queries from size 20 onwards; the same trend is observed for *gStore* too. Further, *Virtuoso* always loses its robustness as the query size increases. On the other hand, AMBER answers queries for all sizes.

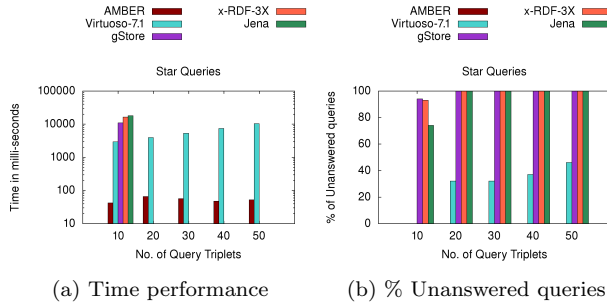


Figure 10: Evaluation of (a) time performance and (b) robustness, for *Star-Shaped* queries on *LUBM100*.

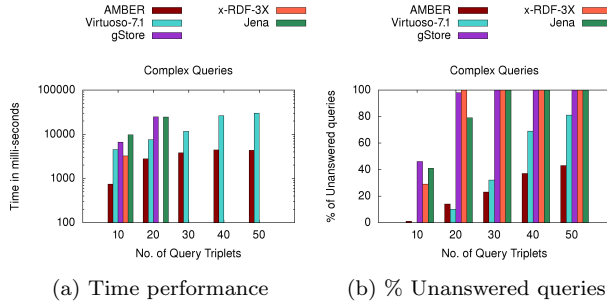


Figure 11: Evaluation of (a) time performance and (b) robustness, for *Complex-Shaped* queries on *LUBM100*.

Considering the results for *Complex-Shaped* queries (Fig. 11), we underline that AMBER has better time performance as seen in Figure 11a. *x-RDF-3X*, *Jena* and *gStore* did not supply answer for size 30 onwards (Fig. 11b). Further, *Virtuoso* seems to be a tough competitor for AMBER in terms of robustness for size 10 and 20. However, for size 30 onwards AMBER is more robust.

To summarise, we observe that *Virtuoso* is enough robust for *Complex-Shaped* smaller queries (10-20), but fails for bigger (>20) queries. *x-RDF-3X* fails for queries with size bigger than 10. *Jena* has reasonable behavior until size 20, but fails to deliver from size 30 onwards. *gStore* has a reasonable behavior for size 10, but its robustness deteriorates from size 20 onwards. To summarize, AMBER clearly outperforms, in terms of time and robustness, the state-of-the-art RDF engines on the evaluated benchmarks and query configuration. Our proposal also scales up better than all the competitors as the size of the queries increases.

## 8. CONCLUSION

In this paper, a multigraph based engine AMBER has been proposed in order to answer complex SPARQL queries over RDF data. The multigraph representation has bestowed us with two advantages: on one hand, it enables us to construct efficient indexing structures, that ameliorate the time performance of AMBER; on the other hand, the graph representation itself motivates us to exploit the valuable work done until now in the graph data management field. Thus, AMBER meticulously exploits the indexing structures to address the problem of sub-multigraph homomorphism, which

in turn yields the solutions for SPARQL queries. The proposed engine AMBER has been extensively tested on three well established RDF benchmarks. As a result, AMBER stands out w.r.t. the state-of-the-art RDF management systems considering both the robustness regarding the percentage of answered queries and the time performance. As a future work, we plan to extend AMBER by incorporating other SPARQL operations and, successively, study and develop a parallel processing version of our proposal to scale up over huge RDF data.

## 9. REFERENCES

- [1] G. A., M. T. Özsu, and K. Daudjee. Workload matters: Why RDF databases need a new design. *PVLDB*, 7(10):837–840, 2014.
- [2] G. Aluç, O. Hartig, M. T. Özsu, and K. Daudjee. Diversified stress testing of RDF data management systems. In *ISWC*, pages 197–212, 2014.
- [3] J. Broekstra, A. Kampman, and F. van Harmelen. Sesame: A generic architecture for storing and querying RDF and RDF schema. In *ISWC*, pages 54–68, 2002.
- [4] E. Cabrio, J. Cojan, A. P. Aprosio, B. Magnini, A. Lavelli, and F. Gandon. Qakis: an open domain QA system based on relational patterns. In *ISWC*, 2012.
- [5] J. J. Carroll, I. Dickinson, C. Dollin, D. Reynolds, A. Seaborne, and K. Wilkinson. Jena: implementing the semantic web recommendations. In *WWW*, pages 74–83, 2004.
- [6] O. Erling. Virtuoso, a hybrid rdbms/graph column store. *IEEE Data Eng. Bull.*, 35(1):3–8, 2012.
- [7] A. Gubichev and T. Neumann. Exploiting the query structure for efficient join ordering in sparql queries. In *EDBT*, pages 439–450, 2014.
- [8] W.-S. Han, J. Lee, and J.-H. Lee. Turbo<sub>iso</sub>: towards ultrafast and robust subgraph isomorphism search in large graph databases. In *SIGMOD*, pages 337–348, 2013.
- [9] J. Huang, D. J Abadi, and K. Ren. Scalable sparql querying of large rdf graphs. *PVLDB*, 4(11):1123–1134, 2011.
- [10] J. Kim, H. Shin, W.-S. Han, S. Hong, and H. Chafi. Taming subgraph isomorphism for RDF query processing. *PVLDB*, 8(11):1238–1249, 2015.
- [11] M. Morsey, J. Lehmann, S. Auer, and A.C.N. Ngomo. Dbpedia sparql benchmark performance assessment with real queries on real data. In *ISWC*, pages 454–469, 2011.
- [12] T. Neumann and G. Weikum. x-rdf-3x: Fast querying, high update rates, and consistency for RDF databases. *PVLDB*, 3(1):256–263, 2010.
- [13] M. Terrovitis, S. Passas, P. Vassiliadis, and T. Sellis. A combination of trie-trees and inverted files for the indexing of set-valued attributes. In *CIKM*, pages 728–737. ACM, 2006.
- [14] L. Zou, R. Huang, H. Wang, J. Xu Yu, W. He, and D. Zhao. Natural language question answering over RDF: a graph data driven approach. In *SIGMOD Conference*, pages 313–324, 2014.
- [15] L. Zou, M. T. Özsu, L. Chen, X. Shen, R. Huang, and D. Zhao. gstore: a graph-based SPARQL query engine. *VLDB J.*, 23(4):565–590, 2014.